

ACS SYMPOSIUM SERIES **561**

Interfacial Design and Chemical Sensing

Thomas E. Mallouk, EDITOR
Pennsylvania State University

D. Jed Harrison, EDITOR
University of Alberta

Developed from a symposium sponsored
by the Division of Colloid and Surface Chemistry
at the 206th National Meeting
of the American Chemical Society,
Chicago, Illinois,
August 22–27, 1993



American Chemical Society, Washington, DC 1994

Contents

Preface.....	xi
1. Chemically Sensitive Interfaces.....	1
D. Jed Harrison and Thomas E. Mallouk	
NEW MATERIALS	
2. Design of Thin Films with Nanometer Porosity for Molecular Recognition.....	16
T. Bein and Y. Yan	
3. Zeolite Synthesis: Can It Be Designed?.....	27
Mark E. Davis	
4. Design, Synthesis, and Characterization of Gated Ion Transporters.....	38
Gordon G. Cross, Thomas M. Fyles, Pedro J. Montoya-Pelaez, Wilma F. van Straaten-Nijenhuis, and Xin Zhou	
5. Langmuir–Blodgett Monolayers as Templates for the Self-Assembly of Zirconium Organophosphonate Films ...	49
Houston Byrd, John K. Pike, Margaret L. Showalter, Scott Whipps, and Daniel R. Talham	
6. Shape-Selective Intercalation and Chemical Sensing in Metal Phosphonate Thin Films.....	60
Louis C. Brousseau, Katsunori Aoki, Huey C. Yang, and Thomas E. Mallouk	
7. High Surface Area Silica Particles as a New Vehicle for Ligand Immobilization on the Quartz Crystal Microbalance	71
Rick Cox, Dario Gomez, Daniel A. Buttry, Peter Bonnesen, and Kenneth N. Raymond	

8. Selective Detection of SO₂(g) at the P-Type Porous Silicon–Gas Interface: Photophysical Evaluation of Interfacial Chemistry	78
Andrew B. Bocarsly, Jonathan K. M. Chun, and Michael T. Kelly	
9. Chemical Sensors and Devices Based on Molecule–Superconductor Structures	91
J. T. McDevitt, D. C. Jurbergs, and S. G. Haupt	
STRUCTURALLY TAILORED INTERFACES	
10. Synthesis and Characterization of Two-Dimensional Molecular Recognition Interfaces	104
Richard M. Crooks, Orawon Chailapakul, Claudia B. Ross, Li Sun, and Jonathan K. Schoer	
11. Channel Mimetic Sensing Membranes Based on Host–Guest Molecular Recognition by Synthetic Receptors...	123
Kazunori Odashima, Masao Sugawara, and Yoshio Umezawa	
12. Passivation and Gating at the Electrode–Solution Interface via Monomolecular Langmuir–Blodgett Films: Mechanism of Alkanethiol Binding to Gold	135
Marcin Majda	
13. Design and Electrochemical Characterization of Lipid Membrane–Electrode Interfaces.....	145
Naotoshi Nakashima and Toshiyuki Taguchi	
14. Molecular Modeling and Chemical Sensor Response.....	155
Michael Thompson, M. Donata Frank, and David C. Stone	
15. Enhanced Metal Nucleation with Self-Assembled Monolayers of ω-Substituted Silanes Studied by Scanning Force Microscopy	162
David J. Dunaway and Robin L. McCarley	
16. Scanning Tunneling Microscopy on a Compressible Mercury Sessile Drop.....	175
Jiri Janata, Cynthia Bruckner-Lea, John Conroy, Andras Pungor, and Karin Caldwell	

- 17. Nucleation and Growth of Molecular Crystals on Molecular Interfaces: Role of Chemical Functionality and Topography 186**
Phillip W. Carter, Lynn M. Frostman, Andrew C. Hillier, and Michael D. Ward
- 18. Organic–Inorganic Molecular Beam Epitaxy: Ordered Monolayers of Phthalocyanines, Naphthalocyanines, and Coronene on Cu (100), SnS₂ (0001), and MoS₂ (0001) 202**
C. D. England, G. E. Collins, T. J. Schuerlein, and N. R. Armstrong
- 19. Surface Sensitivity of Electron Energy Loss Spectroscopy and Secondary-Ion Mass Spectrometry of Organic Films 216**
M. Pomerantz, R. J. Purtell, R. J. Twieg, S.-F. Chuang, W. Reuter, B. N. Eldridge, and F. P. Novak

CHEMICAL SENSOR DESIGNS

- 20. Electroanalytical Strategies with Chemically Modified Interfaces..... 230**
H. D. Abruña, F. Pariente, J. L. Alonso, E. Lorenzo, K. Triple, and S. K. Cha
- 21. Silicon-Based Chemical Microsensors and Microsystems 244**
Elisabeth M. J. Verpoorte, Bart H. van der Schoot, Sylvain Jeanneret, Andreas Manz, and Nico F. de Rooij
- 22. Multilayered Coatings of Perfluorinated Ionomer Membranes and Poly(phenylenediamine) for the Protection of Glucose Sensors In Vivo..... 255**
D. Jed Harrison, Francis Moussy, Stephen Jakeway, Zhonghui Fan, and Ray V. Rajotte
- 23. Chemically Sensitive Interfaces on Surface Acoustic Wave Devices 264**
Antonio J. Ricco, Richard M. Crooks, Chuanjing Xu, and Ronald E. Allred
- 24. Surface and Interfacial Properties of Surface Acoustic Wave Gas Sensors 280**
R. Andrew McGill, J. W. Grate, and Mark R. Anderson

25. Electropolymerized Films in the Development of Biosensors.....	295
Allan Witkowski, Seung-Tae Yang, Sylvia Daunert, and Leonidas G. Bachas	
26. Molecular Interfacing of Enzymes on the Electrode Surface.....	305
M. Aizawa, G. F. Khan, E. Kobatake, T. Haruyama, and Y. Ikariyama	
27. Fluorescent Chemosensors of Ion and Molecule Recognition: Recent Applications to Pyrophosphate and to Dopamine Sensing.....	314
Anthony W. Czarnik	

INDEXES

Author Index	326
Affiliation Index	327
Subject Index	328

Chapter 2

Design of Thin Films with Nanometer Porosity for Molecular Recognition

T. Bein¹ and Y. Yan²

Department of Chemistry, Purdue University, West Lafayette, IN 47907

Chemical sensors based on selective sorption in microporous oxide films are described. Several strategies for the formation of thin films with well-defined sub-nanometer pores are presented. These include the attachment of molecular sieve crystals and organically modified clays on gold substrates. Zeolite crystals are attached to gold electrodes on quartz crystal microbalances *via* molecular anchoring groups, and combined with glass overlayers. In situ nitrogen and organic vapor adsorption studies on the films show that substantial zeolitic microporosity is accessible such that highly selective sensors based on molecular size could be designed. Uptake of molecules small enough to enter the zeolite pores can be one hundred times greater than that of molecules with kinetic diameters greater than the zeolite pores. The selective adsorption can be tailored by variation of the zeolite composition, pore sizes, and other parameters. The selectivity of these stable films was further controlled by ion exchange in the film, effectively incorporating "gate" functions into the layers. The structure and sorptive behavior of the above films will be compared with microporous films based on organically modified clays.

A chemical sensor¹ is a device that can monitor concentrations of gases or liquids *continuously on site* by converting a chemical interaction (mostly on surfaces) into an electronic or optical response. Chemical sensors will play an increasingly important role in environmental monitoring (ground water, plant effluents, waste disposal sites, car exhaust), automated manufacturing processes, and medical monitoring. The ability to continually measure important parameters in these and other applications will be the key to greater efficiency, time- and energy-savings, and environmental safety and health in the industry of the coming decades. For example, it will be much more efficient to place *in-situ* sensors in the periphery of a waste disposal site to monitor

¹Current address: YTC America, Inc., 550 Via Alondra, Camarillo, CA 93012

toxic effluents and ground water quality instead of collecting soil samples that have to be analyzed individually in a central laboratory.

A number of physical devices with chemical sensitivity have been developed previously, including the quartz crystal microbalance (QCM) and other acoustic wave devices, semiconductor gas sensors, and various chemically sensitive field effect transistors. However, based on their intrinsic detection principles, most of the known solid state chemical sensors are not selective, i.e., they respond to more than one or a few chemical species. There is an urgent demand for new families of selective, microscope sensors that can eventually be integrated into microelectronic circuits. We have embarked on a program aimed at the design of *conceptually new microporous thin films with molecular recognition capabilities*. On the surface of chemical sensors, these membranes will serve as "molecular sieves" that control access of selected target molecules to the sensor surface.

Piezoelectric acoustic wave device such as the quartz crystal microbalance² offer many attractive features as vapor phase chemical sensors: small size, ruggedness, electronic output, sensitivity, and adaptability to a wide variety of vapor phase analytical problems.³ The QCM is based on a piezoelectric quartz substrate coated with keyhole pattern electrodes on opposite surfaces on the crystal. Mass changes Δm (in g) per face of the QCM cause proportional shifts Δf of the fundamental resonance frequency F , according to

$$\Delta f = -2.3 \times 10^{-6} F^2 \Delta m/A$$

where A is the electrode surface area (in cm^2). It follows that the 9 or 5 MHz QCM is capable of detection of mass changes at the nanogram level.^{4,5,6}

Zeolite molecular sieves are crystalline, porous inorganic solids, typically aluminosilicates, with channel diameters ranging from 0.3 to 1.2 nm and beyond, and crystal sizes typically between 0.5 and 5 μm .^{7,8} If species are selectively adsorbed into the well-defined channel systems of zeolites, the sensor response can be made selective for those species, while larger molecules are only adsorbed on the outer surface of the sensor membrane. Furthermore, many zeolites show ion exchange capability which introduces numerous possibilities for intrapore modifications.

Experimental

Porosity characterization of the thin films.

Nitrogen sorption isotherms. These were obtained at liquid nitrogen temperature in a computer-adjusted mass flow controller system (Unit Instruments Inc.). Nitrogen partial pressures in helium were adjusted over the range of 0-0.95. QCMs coated with zeolite and clay thin films were usually pretreated at 200°C in helium for 2 h. The zeolites were dehydrated under these conditions, as shown by stabilization of the QCM frequency and from related FTIR experiments of similar films. Data acquisition and analysis was performed with DAS-16 analog-digital I/O boards (Keithley Metrabyte Co.). The frequency changes of the coated QCMs upon nitrogen

sorption/desorption and the nitrogen partial pressures were monitored at intervals of one second.

Dynamic vapor sorption kinetics and isotherms. Different vapor concentrations were generated with gravimetrically calibrated vapor diffusion tubes at 25°C under constant flow of carrier gas (15 ml/min helium). Vapor concentrations were adjusted by dilution with a second computer controlled helium flow (0-200 ml/min). Sorption measurements were carried out similar to those described above for nitrogen. Equilibrium was usually assumed and the next partial pressure was adjusted when the frequency change of the QCM was less than 1 Hz in 90 seconds. The close coincidence of adsorption and desorption branches of many isotherms shows that the measurements are often close to true equilibrium.

Results and Discussion

Zeolite Single Layers Attached through Molecular Coupling Agents. Our recent development of molecular sieve-based composite films has introduced a novel means for tailoring vapor/surface interactions.⁹⁻¹⁵ Our initial approach was focused on zeolite/glass microcomposites derived from sol/gel suspensions that were coated on surface acoustic wave devices. However, even though zeolite/glass composites have favorable stability and show zeolite microporosity, the glass matrix can introduce some additional nonselective porosity and/or obstruct part of the zeolitic porosity.

An alternative means of attachment is a monolayer of a reactive coupling agent that can bind the zeolite crystals to the sensor surface. The coupling agent 3-mercaptopropyl-trimethoxysilane, $\text{HS}(\text{CH}_2)_3\text{Si}(\text{OCH}_3)_3$, was used as a bifunctional molecular precursor for anchoring zeolite crystals to the gold electrode.^{11,15} Gold shows strong specific interactions with thiol groups that permit formation of self-assembled monolayers in the presence of many other functional groups.¹⁶⁻¹⁸ Figure 1 summarizes the idealized process of the formation of a zeolite-coated QCM. A related system consisting of SnO_2 /cationic disilane/zeolite arrangements has been reported for the self-assembly of redox chains on electrodes.¹⁹

Adsorption of many organic vapors, including small alcohols, chlorinated hydrocarbons, benzene, toluene, as well as water was demonstrated in these films. Dynamic sorption isotherms of organic vapors and nitrogen as well as the transient sorption behavior of organic vapor pulses were studied to characterize the zeolite-coated QCMs. The regular micropores (0.3-0.75 nm) of the QCM-attached zeolite crystals were found to efficiently control molecular access into the coating. Selectivity of the frequency response in excess of 100:1 towards molecules of different size and/or shape (molecular sieving) could be demonstrated.

The thin films can equilibrate and desorb vapors within a few seconds to minutes, often at room temperature, while the bulk materials need substantial heating (ca. 200-300°C) to remove the absorbed vapors (the last ppm desorption steps of water from polar zeolite films at r.t. can take 30-50 min). Thus the sensor response occurs at a satisfactory time scale. The kinetics of vapor desorption from the zeolite layers are strongly dependent on the adsorbate/zeolite combination, thus providing an additional capability for molecular recognition.

Ethanol sensor. As indicated above, zeolites discriminate molecules not only based on size but also by the strength of surface interactions (heat of adsorption). We

demonstrate that silicalite-based films on QCMs show selective response towards ethanol in competition with water and larger organics such as 2,2,3-trimethylpentane.¹² The preparation of the microporous layer involved two steps: First, silicalite crystals (about 3 μm diameter) were chemically anchored to the QCM gold electrodes via a thiol-organosilane coupling layer. Silicalite is a crystalline molecular sieve of approximate composition SiO_2 with a pore system of zig-zag channels along A (free cross-section ca. 5.1 x 5.5 \AA), linked by straight channels along B (5.3 x 5.6 \AA).²⁰ The silicalite crystals bonded to the QCM electrodes were then further coated with an amorphous, porous silica layer, prepared via sol-gel processing from $\text{Si}(\text{OEt})_4$. The films have the following typical adsorption characteristics: Saturation of the micropores at 20°C (derived from α -plots) was achieved with 0.12 $\mu\text{g}/(\mu\text{g}$ film) of ethanol, corresponding to a microporosity of 0.15 cm^3/g .

The selective vapor responses of the QCM coated with the silicalite composite layer are illustrated by the sorption of pure vapors of ethanol (ca. 4.3 \AA diameter), 2,2,3-trimethylpentane (iso-octane, ca. 6.2 \AA) and water (2.65 \AA) in the range of 0-2000 parts per million (ppm) in moles (Figure 2). The sorption of ethanol (top curve) shows the largest and fairly linear response as a function of vapor concentration. In contrast, the response of the sensor to iso-octane (bottom line) exhibits an almost negligible change with increasing vapor concentration. Exclusion of 2,2-dimethylbutane from the microporous coating was also observed. The results show that novel sensing layers with highly effective molecular sieving functions and very low external surface areas can be designed. Sorption of the small water molecules (middle line) shows also a small response. Although water sorption slightly increases with increasing concentration, it already approaches a rectilinear isotherm at these low concentrations. This behavior differs drastically from the sorption of ethanol.

The nature of the hydrophobic sensing layer and the preferential adsorption of ethanol over water on a pre-loaded (7% water, which appears to block strongly adsorbing defect sites) QCM can be understood by evaluating the isosteric heats of absorption.²¹ Water sorption on a polar surface is through specific interactions with cations or hydroxyls. When such energetic sites (cations) are "blocked" by molecules presorbed in the silicalite layer, the isosteric heat of adsorption of water over the range of 8-14 $\text{ng}/\mu\text{g}$ in the sensing layer is about 6.6 kcal mol^{-1} , substantially below that of the heat of liquefaction of water (10.5 kcal mol^{-1} at 25°C) and similar to that reported for pure silicalite. Thus it is energetically unfavorable for water to condense into such a system. In contrast, for ethanol an isosteric heat of 11 kcal mol^{-1} is obtained over a wide sorption range of 20-80 $\text{ng}/\mu\text{g}$. This value is *greater* than the heat of liquefaction of ethanol (10.1 kcal mol^{-1} at 25°C). The favorable sorption of ethanol vs. water also illustrates that pronounced micropore filling by ethanol can occur at low concentrations. Some initial competitive measurements of ethanol with other vapors confirm the high selectivity discussed above.¹²

Gate functions. An intriguing possibility exists to manipulate adsorption into the zeolite-based films by appropriate gate functions. If molecular entry into the zeolite pore volume is controlled on the crystal surface or inside the crystal, one can "switch" the selectivity from one molecular size to another. We demonstrate this concept with the example of zeolite A, the well-known material used to dry solvents.²² The eight-ring openings of zeolite A into its large cage have a diameter of only about 4.5 \AA . When this zeolite is exchanged with large, singly-charged cations, the free opening

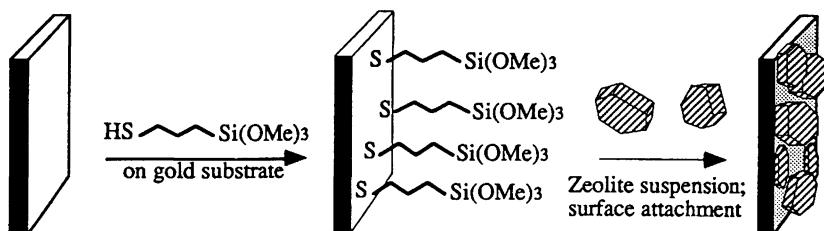


Figure 1. Anchoring process of zeolite crystals on a gold surface *via* a thiol-alkoxysilane layer.

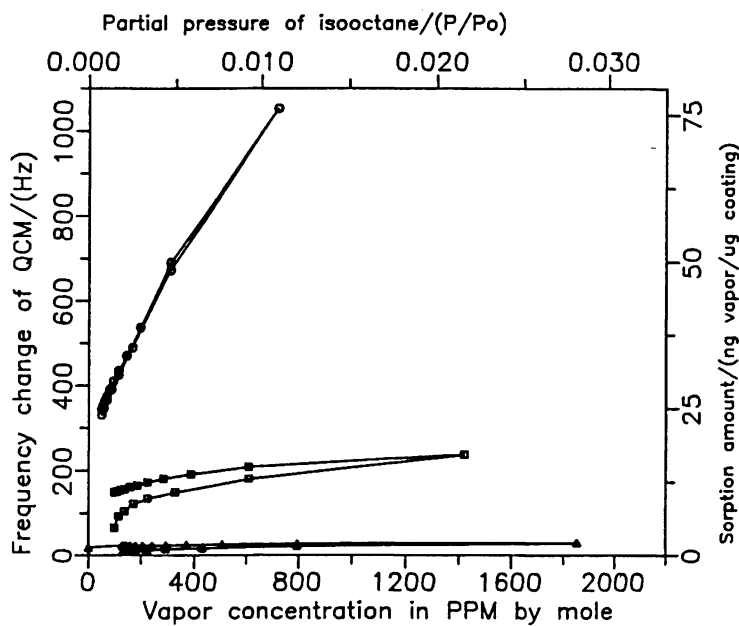


Figure 2. Sorption isotherms at 20°C of ethanol (o), water (squares) and isooctane (Δ) on a QCM coated with silicalite/silica composite. From ref. 12. The QCM frequency shifts in this and the following plots were multiplied with (-1).

is narrowed and the molecular selectivity changes. Thus, zeolite 5A contains Ca(II), 4A contains Na(I), and 3A is the potassium form. The numbers indicate the approximate effective pore openings in Å.

Piezoelectric devices (QCMs) were coated with the Ca-form of zeolite A, using a bifunctional thiol-monolayer for attachment as described above. This film shows a Type I nitrogen sorption isotherm indicating microporosity accessible to nitrogen, as expected for this zeolite. In order to switch the film to a different selectivity, the entire QCM was submerged in dilute Na(I), K(I), or Rb(I) solutions. Ion exchange could be demonstrated by the weight change of the film. Nitrogen sorption isotherms are extremely sensitive to this treatment: the Na-form is already almost completely blocked (sorption is extremely slow), while no nitrogen sorbs in the K(I) and Rb(I) forms. Accordingly, the sorption isotherms corresponding to the latter status of the film are Type II with only external sorption. These changes in pore opening become even more obvious when organic vapors are sorbed in the different versions of the films. For example, the Ca-form sorbs water (2.7 Å), ethanol, and n-hexane, while the Na-form already shuts down for hexane (4.3 Å), and sorbs ethanol (4.3 Å) only weakly. A film highly selective for only water is formed when it is exchanged with potassium ions (Figure 3). Ethanol, hexane, and other larger hydrocarbons are effectively excluded from this film (Figure 4). These dramatic changes show the powerful control of sorption into such films by simply exchanging the charge-balancing cations of the zeolite structure.

Immobilization of Organoclays on Piezoelectric Devices. Organoclays (layered silicate materials ion-exchanged with alkyl ammonium cations) are interesting complements to zeolite sorbents because their sorption selectivities can be controlled to a large extent by the choice of layer charge density, and structure and chain length of the alkylammonium ions.²³⁻²⁷ Different combinations of these factors will produce very different interlayer environments, containing polar mineral surfaces, hydrophobic organic chains, and paraffin-like layers. The organoclays can offer preferential sorption of nonpolar and flat molecules (Figure 5).

The host discussed in the following was hectorite of approximate composition $\text{Na}_{0.3}(\text{Li}_{0.3}\text{Al}_{0.01}\text{Mg}_{2.67})\text{Si}_4\text{O}_{10}(\text{OH})_2$, with cation exchange capacity of 8 meq/10 g, and charge density of *ca.* one monovalent cation per 100 Å². Hectorite is a layered material of the smectite family, having two tetrahedral silicate sheets fused to an edge-sharing octahedral sheet containing Mg and Li. Intercalation was achieved by exchanging 3 times with three-fold excess (based on cation exchange capacity) with tetramethylammonium (TMA) chloride, tetrapropylammonium (TPrA) bromide and tetrapentylammonium (TPeA) bromide, respectively. Intercalation of long-chain organic cations (3-fold excess) was carried out 3 times in 30% acetonitrile/water solutions of trimethyloctadecylammonium (TrMOA) bromide, dimethyloctadecyl-ammonium (DMDOA) bromide and methyltrioctadecylammonium (MTrOA) bromide, followed by washing in water until bromide-free. The coatings on the QCMs with 6 MHz resonance frequency were formed by dipping the crystals in the respective water or chloroform suspensions of the intercalated silicates. The films were heated at 200°C in nitrogen overnight.

The effect of intercalating various alkylammonium cations into the hectorite host is to increase the interlayer spacing of the Na-form (2.8 Å when partially hydrated) to 4.2, 4.9, and 5.5 Å, when TMA, TPrA, and TPeA ions are intercalated,

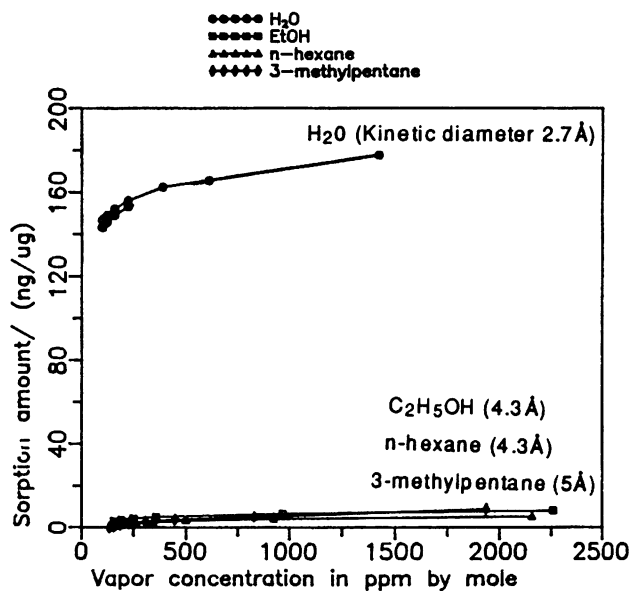


Figure 3. Sorption isotherms at 20°C of water (o), ethanol (squares), n-hexane (Δ) and 3-methylpentane (rhombus) on a QCM coated with potassium-exchanged zeolite A/silica composite.

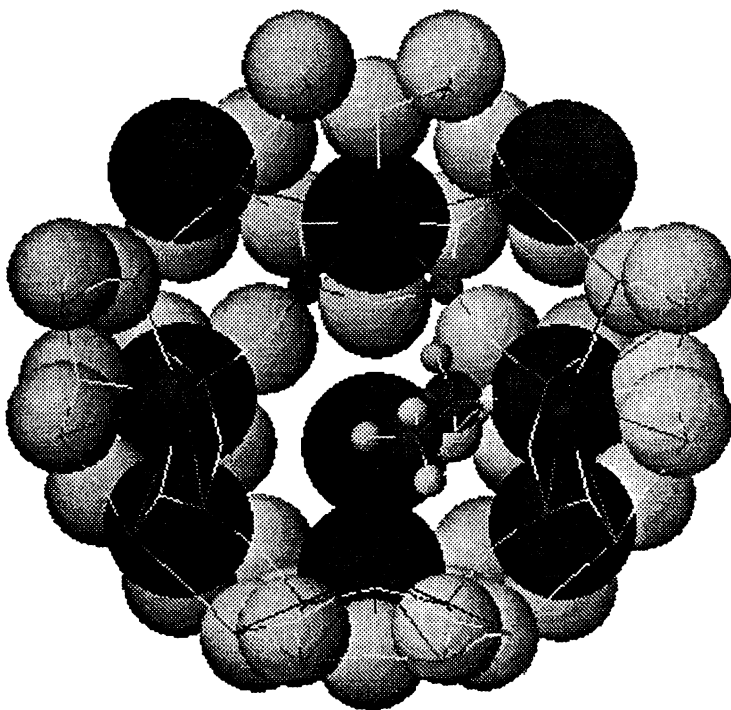


Figure 4. View into the eight ring of potassium-exchanged zeolite A. The blocked path of an ethanol molecule is shown.

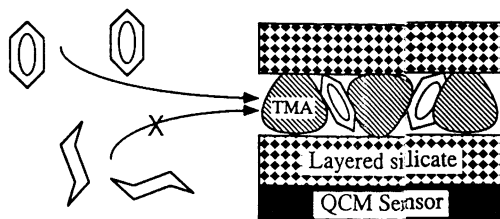


Figure 5. Schematic representation of selective benzene vs. cyclohexane sorption in a TMA-hectorite film on a QCM sensor. From ref. 14.

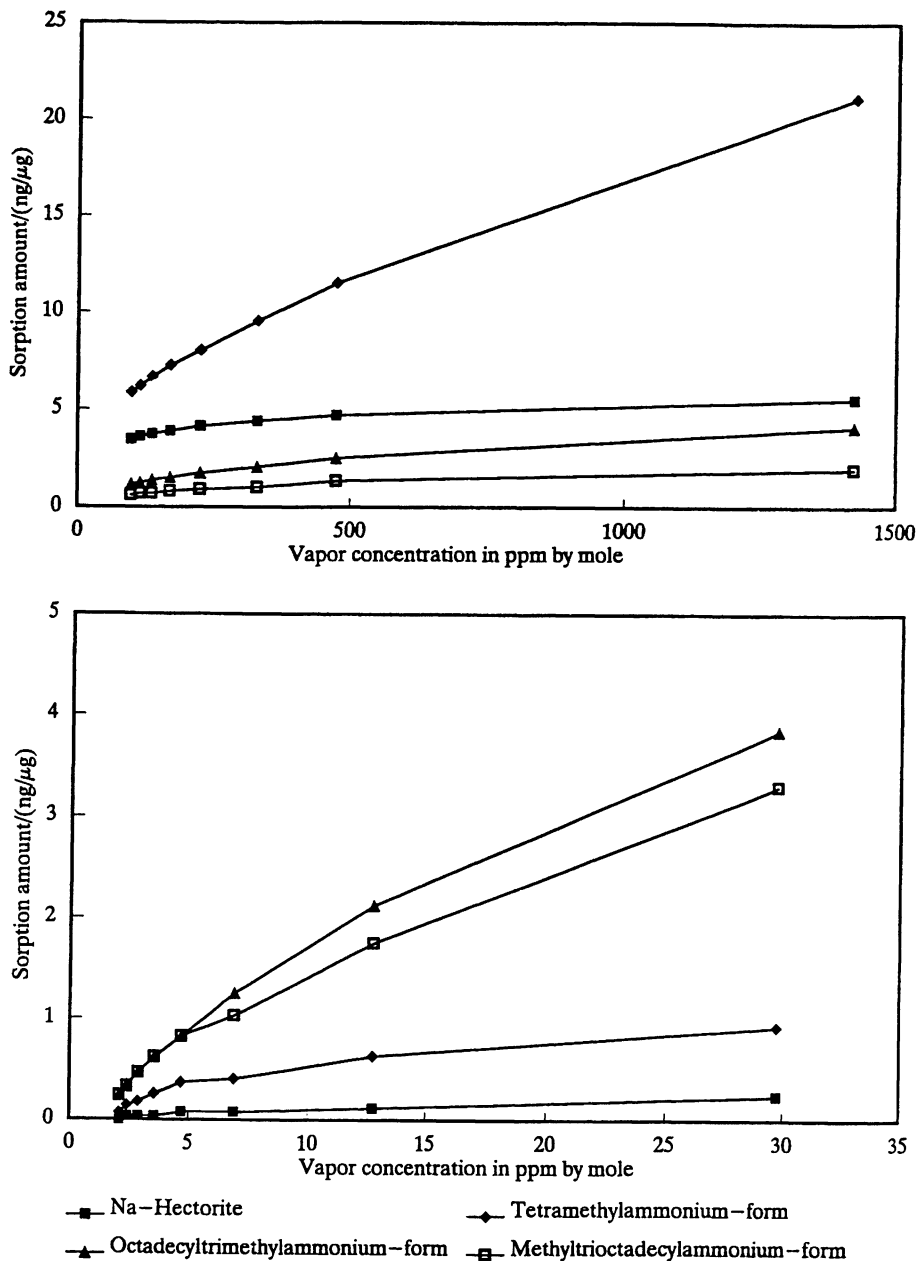


Figure 6. Vapor sorption isotherms at 25°C on Na and alkylammonium forms of hectorite. (A) water sorption (top). (B) toluene sorption (bottom).

respectively. These increased interlayer spacings are due to about one layer of hydrocarbon chains between the sheets of the clay mineral (9.6 Å thick). Intercalation of TrMOA results in an interlayer spacing of 11.1 Å, indicating 2-3 layers of hydrocarbon chains parallel to the clay sheets.²⁸ Finally, when the areal density of octadecyl chains is doubled (dimethyldioctadecylammonium, DMDOA, 21.1 Å) or tripled (methyltrioctadecylammonium, MTrOA, 24.5 Å), they are forced to orient almost normal to the clay sheets, in a paraffinic arrangement similar to Langmuir films.

Nitrogen sorption in the Na- and TMA-forms follows Type I isotherms and clearly shows microporosity for nitrogen with 1.2 and 2.0 wt% of nitrogen in the pores (derived from t-plots with the TPrA film as reference). The latter films show also significant external surface area. In contrast, all other organoclays show Type II isotherms and no microporosity. Vapor sorption isotherms at low partial pressures provide detailed information on the selective sorption behavior. Water sorption in the organoclays most closely tracks that of nitrogen (Figure 6A). The interlayer cavities produced on intercalation of TMA strongly sorb water at 25°C. Less water is sorbed in the Na-form and even less in the TrMOA and MTrOA forms. This behavior can be associated with the hydrophobic nature of the interlayer phase in the two latter organoclays.

A drastic reversal of the selectivities is observed when hydrocarbons are sorbed in the organoclays. Cyclohexane sorption is now most favored in the TrMOA form, and in the following sequence in the other sorbent films: MTrOA > TMA > Na-form. As shown in Figure 6B, toluene (and benzene) are absorbed even more strongly in the organoclays. We associate this increase over the sorption of more saturated six-rings with the compact, flat shape of the aromatics that should allow the molecules to slip into the gaps between the hydrocarbon chains of both the trimolecular horizontal TrMOA structure and the paraffinic more vertical MTrOA structure (relative to the clay sheets). Benzene shows also surprisingly high sorption in the TMA form. The benzene molecule can just barely be accommodated in this form when in a tilted upright orientation, as discussed by Barrer.²⁴ Liquid-like phases with different densities might occur at high loadings but are considered unlikely at the low loadings present in our measurements. Another driving force resulting in the preferred sorption of aromatics could be their higher polarizability. This could play a role in the interactions with organoclays containing TMA, but much less so in the long hydrocarbon (C₁₈) chain systems. There is less sorption of toluene than benzene which could be due to less efficient packing. In summary, the interplay of size exclusion from rigid pores and sorption (partitioning) into the organic phases can cause unique selectivities in the organoclays that complement the molecular sieving of porous framework hosts such as zeolites.

This overview shows the rich variety of sorption behavior of microporous solids that can be combined with piezoelectric devices to create selective sensors. Future work will explore additional parameters such as acid base reactions and coordination chemistry, as well as issues including chemical interferences under real world conditions.

Acknowledgments. The authors appreciate funding for different aspects of this work from the National Science Foundation, and from the U.S. Department of Energy (New

Mexico WERC Program). We thank Drs. Kelly Brown, C. Jeffrey Brinker, and Gregory C. Frye for their contributions to this program.

Literature Cited

1. *Biosensors and Chemical Sensors*, Edelman, P.G.; Wang, J., Editors, ACS Symp. Ser. 487, ACS: Washington, D.C., **1992**.
2. Ward, M.D.; Buttry, D.A., *Science*, **1990**, *249*, 1000.
3. Guilbault, G.G.; Kristoff, J.; Owen, D. *Anal. Chem.* **1985**, *57*, 1754.
4. King, W.H. *Anal. Chem.*, **1964**, *36*, 1735.
5. Hlavay, J.; Guilbault, G.G. *Anal. Chem.*, **1977**, *49*, 1892.
6. Ballantine, D.S.; Wohltjen, H. *Anal. Chem.*, **1989**, *61*, 704A.
7. Breck, D.W. *Zeolite Molecular Sieves*, Krieger: Malabar, Florida, **1984**.
8. Barrer, R.M. *Hydrothermal Chemistry of Zeolites*, Academic Press: London, **1982**.
9. Bein, T.; Brown, K.; Frye, C.G.; Brinker, C.J. *J. Am. Chem. Soc.*, **1989**, *111*, 7640.
10. Bein, T.; Brown, K.; Brinker, C.J., *Zeolites: Facts, Figures, Future*, in P.A. Jacobs, R. A. Van Santen (Eds.), *Stud. Surf. Sci. Catal.* **49**, Elsevier: Amsterdam, **1989**, pp 887.
11. Yan, Y.; Bein, T. *J. Phys. Chem.* **1992**, *96*, 9387.
12. Yan, Y.; Bein, T. *Chem. Mater.* **1992**, *4*, 975.
13. Bein, T.; Brown, K.; Frye, C.G.; Brinker, C.J., U.S. Patent No. 5,151,110, Sept. 29, **1992**.
14. Yan, Y.; Bein, T.; *Chem. Mater.* **1993**, *5*, 905.
15. Yan, Y.; Bein, T.; *Microporous Materials*, **1993**, *1*, 401.
16. Bain, C.D.; Troughton, E.B.; Tao, Y.T.; Evall, J.; Whitesides, G. M.; Nuzzo, R. G. *J. Am. Chem. Soc.* **1989**, *111*, 321.
17. Wasserman, S.R.; Biebuyck, H.; Whitesides, G.M. *J. Mater. Res.*, **1989**, *4*, 886.
18. Porter, M.D.; Bright, T.B.; Allara, D.L.; Chidsey, C.E.D. *J. Am. Chem. Soc.*, **1987**, *109*, 3559.
19. Li, Z.; Lai, C.; Mallouk, T.E. *Inorg. Chem.*, **1989**, *28*, 178.
20. Flanigen, E.M.; Bennett, J.M.; Grose, R.W.; Cihon, J.P.; Patton, R.L.; Kirchner, R.M.; Smith, J.V., *Nature*, **1978**, *271*, 512.
21. The isosteric heats were obtained from the sorption isotherms in the range of 0-40°C by the relation: $Q_{st} = RT_1T_2 \ln(P_1/P_2) / (T_1 - T_2)$, where P_1 and P_2 are the equilibrium concentrations for the same sorption amount in the sensing layer, a, at the temperatures T_1 and T_2 , respectively.
22. Yan, Y.; Bein, T., to be published.
23. Barrer, R.M. *Phil. Trans. R. Soc. Lond.* **1984**, *A 311*, 333.
24. Barrer, R.M.; Perry, G.S. *J. Chem. Soc.* **1961**, 850.
25. Lee, J.-F.; Mortland, M.M.; Boyd, S.A.; Chiou, C.T. *J. Chem. Soc.; Faraday Trans. 1*, **1989**, *85*, 2953.
26. Lee, J.-F.; Mortland, M.M.; Chiou, C.T.; Kile, D.E.; Boyd, S.A. *Clays Clay Min.* **1990**, *38*, 113.
27. Lao, H.; Latieule, S.; Detellier, C. *Chem. Mater.* **1991**, *3*, 1009.
28. Lagaly, G. *Solid State Ionics* **1986**, *22*, 43.